ENGINEERING & TECHNOLOGY SCIENTIFIC JOURNAL

ORIGINAL

2023, VOL. 01, N°. 01, e023001
DOI: 10.55977/etsjournal.v01i01.e023001

Whirl-flutter control through the direct piezoelectric effect

Sérvio Túlio Suenai Haramura Bastos* [1] and Rui Marcos Grombone de Vasconcellos [1]

[1] Universidade Estadual Paulista – Campus de São João da Boa Vista. São João da Boa Vista, 13876-750, São Paulo, Brasil.

Received 2022-07-22
Revised 2022-07-29
Accepted 2022-08-04
Published 2023-03-23

***Corresponding author**
Sérvio T. S. H. Bastos
tulio.haramura@unesp.br

***ORCID**
0000-0003-2448-7899

Page e-location ID
e023001

Distributed under
CC BY-NC 4.0

Copyright: Authors
OPEN ACCESS

ABSTRACT

The aeroelastic instability known as whirl-flutter must be considered during the design of a propeller-driven aircraft. Usually, aircraft with single or multiple rotors may suffer from such a phenomenon, mainly when a large rotor diameter is applied, such as vertical take-off and landing aircraft (VTOL) with or without tilt rotors. Depending on the cruise speed, the whirl-flutter influences the rotors, wings, and pylons project. With the advent of modern air mobility, a better understanding of the such phenomenon and the development of vibrational control techniques to increase the stability margins becomes essential. Although intelligent materials, such as piezoceramics, are commonly applied to control aeroelastic phenomena, the application to whirl-flutter management still needs to be investigated. Thus, the present research proposes a passive control technique based on the direct piezoelectric effect in *unimorph* and *bimorph* harvester configurations, observing its impact on the aeroelastic system's behavior. As the main result of the piezoelectric material presence, an increased flutter speed is monitored, improving the system's stability. Additionally, the *bimorph* configuration is more efficient in postponing the critical speed.

Keywords Whirl-flutter; Passive control; Direct piezoelectric effect; *Unimorph* harvester; Bimorph harvester.

1. INTRODUCTION

Intelligent materials can couple several physical domains. Such coupling is observed when a determined physical domain state variable influence others (Anicezio, 2015). Due to such a material's ability, environmental changes could be explored to activate its extrinsic or intrinsic functions (Akhras, 2000). In the case of piezoelectrics or piezoceramics (PZT), which are the focus of the present research, there is a coupling between the electrical and mechanical domains (Anicezio, 2015).

The choice of such material lies on the necessity of alternative forms to produce electrical energy to feed low-powered consumption devices, such as microelectromechanical systems and actuators (Muralt, 2000), health monitoring sensors, and wireless sensors (Roundy & Wright, 2004), medical implants (Karami & Inman, 2012) and cameras (Abdelkefi & Ghommem, 2013). Energy Harvesting rises to its purposes and may be defined as the process in which light, solar, thermal, and kinetic energies can be converted to electrical ones to power several electronic devices with low power consumption. Nonetheless, mechanical conversion is the most explored once such a type can be found, even when the thermal or light energies are absent (Abdelkefi, 2016).

Aeroelastic instabilities rise as an essential and exciting form to obtain electrical energy from mechanical vibrations since structures, when submitted to a flow, may suffer different types of dynamical responses; thus, the mechanical-electrical conversion is possible and practical (Vasconcellos & Abdelkefi, 2015). Chimneys, transmission lines, pipelines or rises, landing gear, wings, and aircraft rotors are susceptible to them. They may be damaged due to fatigue or other structural damages related to high amplitude oscillations, causing possible severe structural failures and, as a consequence, economic and environmental losses (Bastos, Vasconcellos & Marques, 2019a, 2019b).

Several research has been done to model, prevent, and analyze aeroelastic behavior in different structures, including vibration control and energy harvesting, by applying piezoelectrics. De Marqui Jr, Erturk & Inman (2009) analyzed how the piezoelectric effects influence the aeroelastic flutter instability, Abdelkefi, Nayfeh & Hajj (2011) observed how the aerodynamic and structural nonlinearities affect a piezo-aeroelastic wing system, Abdelkefi, Hajj & Nayfeh (2012) investigate the effects of different cross-sections geometries on galloping oscillation and energy harvesting, D'Assunção (2013) performed studies to control and energy harvesting for a typical aeroelastic section, Silva (2014) assessed different types of piezoelectric controllers for aeroelastic systems, Anicezio (2015) the semi-passive control on helicopters blades, Naseer, Dai, Abdelkefi & Wang (2017) assessed the magnetic nonlinear effects on both the piezoelectric energy harvesting and the aeroelastic behavior in a cylinder submitted to vortex-induced vibration (VIV) and Bastos & Vasconcellos (2021) performed an analysis on piezoelectric energy harvesting and amplitude attenuation in a cylinder submitted to VIV.

Even though all types of aeroelastic instabilities have their importance, focusing on the aeronautical branch, flutter instability is the most important. It is

featured as dynamical aeroelastic instability in which aerodynamic, inertial, and elastic forces interact in a fixed or rotating wing. Due to such interaction, the energy provided by the fluid is transferred to the structure, causing a divergent response (Latif, Khan, Javed, Shah & Rizvi, 2021). When a critical speed, commonly denoted as flutter speed, is reached, the vibrational motion becomes self-excited due to insufficient damping compared to the non-stationary aerodynamic loads (Abdelkefi, 2016). Such movements could cause catastrophic failures in aeronautical structures and received special attention from researchers.

Considering the next generation of propeller-driven aircraft, such as turboprop and vertical take-off and landing (VTOL) as tilt rotors, as depicted in **Fig. 1**, an essential subtype of flutter becomes significant, the whirl-flutter (Adeyemi, Cleaver & Du Bois, 2019). It has been identified by Taylor & Browne (1938) and primarily analyzed by Ribner (1945a, 1945b), but only in 1959 and 1960 with *Lockheed L-188 C Electra I* accidents was its importance recognized. The whirl-flutter provides a divergent elliptical precession motion that occurs in the aircraft's rotor due to the structural, aerodynamic, and gyroscopic effect combination, which promotes non-stationary aerodynamic forces and moments causing high amplitudes of oscillation that may damage the rotor's mount and possibly the pylons, wings and other aircraft's structures (Čečrdle, 2015). When the airspeed exceeds the critical speed, the divergent precession movement may occur from the forward (FW) and backward (BW) modes. The FW mode is characterized by higher frequency and precession in the same direction as the rotor's angular velocity. The BW mode has a lower frequency and precession velocity when compared with the FW mode, in the opposite direction as the rotor's angular velocity. The instability will occur only in BW mode considering the blades are rigid bodies. Nonetheless, if blade flexibility is introduced, the whirl-flutter phenomenon may occur in both modes (Čečrdle, 2015).



Figure 1. CV-22B Osprey. Source: Extracted from Adeyemi et al. (2019).

Given its importance and the need for structural optimization, a better understanding of the system's behavior, and the development of control

techniques, several recent research have been done. Piatak et al. (2003); Mueller, Gourinat, Ferrer & Kerdreux (2004); Kruger (2016); Adeyemi et al. (2019) and Liu Xu (2020) have observed the aeroelastic and aerodynamic system's behavior as well as active vibration control. Additionally, Mair, Rezgui & Titurus (2018, 2019), Mair, Titurus & Rezgui(2021), and Quintana, Vasconcellos, Throneberry & Abdelkefi (2021) have analyzed the nonlinear structural effects on the system's behavior. However, there is a gap regarding the effects of piezoceramics on the aeroelastic behavior of a system submitted to whirl-flutter.

Considering the importance of the whirl-flutter prediction and control to the actual aeronautical scenario and the possibility of piezoelectric materials application as an effective strategy to control this instability, the present research proposes a passive control technique applying piezoelectric transducers in a *unimorph* and *bimorph* configurations in order to increase the stability margin of aeroelastic systems subjected to whirl flutter, contributing to the development of safe and lighter aircraft.

2. AEROELASTIC MODEL

The applied mechanical model in the present research is based on the formulation described by Reed III (1966) and Bielawa (2005) and used by Mair et al. (2018), Quintana et al. (2021), and Bastos & Vasconcellos (2022a, 2022b). They are considering a lumped model with two degrees of freedom (2DOF), representing the pitch and yaw rotor's movements defined as θ e ψ. Also, consider that the rotor with a radius R and an inertia I_x is connected at a distance an R from the aircraft structure and is submitted to an axial airflow U parallel to axis x. Besides that, the nacelle moment of inertia is given as I_n, and the wing structure contributions are modeled as equivalent stifflowness, k_θ and k_ψ, and damping, c_θ and c_ψ, in both DOF. Thus, the system may be represented in **Fig. 2**.

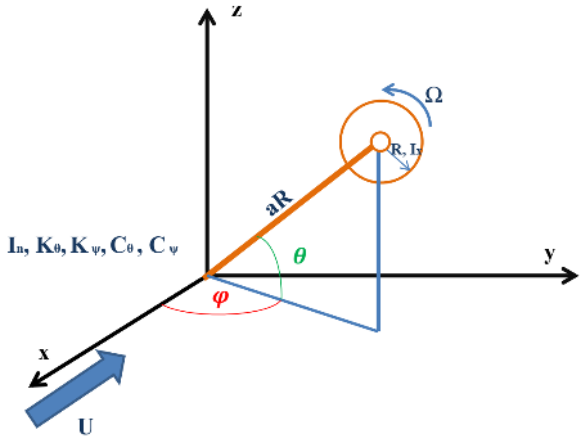


Figure 2. A rotor-nacelle schematic system with 2DOF to whirl-flutter instability.

The governing **Equations (1 – 12)** of the system depicted in **Fig. 2** are given by:

$$\begin{bmatrix} I_n & 0 \\ 0 & I_n \end{bmatrix} \begin{Bmatrix} \ddot{\theta} \\ \ddot{\psi} \end{Bmatrix} + \begin{bmatrix} c_\theta & -I_x\Omega \\ I_x\Omega & c_\psi \end{bmatrix} \begin{Bmatrix} \dot{\theta} \\ \dot{\psi} \end{Bmatrix} + \begin{bmatrix} k_\theta & 0 \\ 0 & k_\psi \end{bmatrix} \begin{Bmatrix} \theta \\ \psi \end{Bmatrix} = \begin{Bmatrix} M_\theta \\ M_\psi \end{Bmatrix} \quad \textbf{(Eq. 1)}$$

Where M_θ e M_ψ are, respectively, the pitch and yaw aerodynamics moments obtained by Ribner (1945b) applying the *Blade element theory* with *quasi*-steady aerodynamics in which forces and moments only depend on the rapid body movements neglecting the fluid movement and the wake influence (Bielawa, 2005), so, such moments are described as follows:

$$M_\theta = \frac{n_b k_a R}{2}\left[-(A_3 + a^2 A_1)\frac{\dot{\theta}}{\Omega} - A_2'\psi + aA_1'\theta\right] \quad \textbf{(Eq. 2)}$$

$$M_\theta = \frac{n_b k_a R}{2}\left[-(A_3 + a^2 A_1)\frac{\dot{\psi}}{\Omega} + A_2'\theta + aA_1'\psi\right] \quad \textbf{(Eq. 3)}$$

where $k_a = 0.5\rho c_{l,\alpha} R^4 \Omega^2$, for concise notation. The term ρ is the air density, and cl,α is the blade lift coefficient slope. Furthermore, the Ai terms are the aerodynamics integrals that rise from the lift integration along each blade, defined as:

$$A_1 = \frac{c}{R}\int_0^1 \frac{\mu^2}{\sqrt{\mu^2+\eta^2}}\,d\eta \quad \textbf{(Eq. 4)}$$

$$A_1' = \mu A_1 \quad \textbf{(Eq. 5)}$$

$$A_2' = \frac{c}{R}\int_0^1 \frac{\mu^2\eta^2}{\sqrt{\mu^2+\eta^2}}\,d\eta \quad \textbf{(Eq. 6)}$$

$$A_3 = \frac{c}{R}\int_0^1 \frac{\mu^4}{\sqrt{\mu^2+\eta^2}}\,d\eta \quad \textbf{(Eq. 7)}$$

$$\mu = \frac{U}{\Omega R} \quad \textbf{(Eq. 8)}$$

Bringing over the right-hand side in the left-hand side of **Eq. 1**, the state space form is written as:

$$\dot{\boldsymbol{X}} = \boldsymbol{J}\boldsymbol{X} \quad \textbf{(Eq. 9)}$$

With $\boldsymbol{X} = [\theta, \psi, \dot{\theta}, \dot{\psi}]^T$ and $\boldsymbol{J}$, the Jacobian matrix given by:

$$\boldsymbol{J} = \begin{bmatrix} \boldsymbol{0} & \boldsymbol{I} \\ -\boldsymbol{M}^{-1}\boldsymbol{K} & -\boldsymbol{M}^{-1}\boldsymbol{C} \end{bmatrix} \quad \textbf{(Eq. 10)}$$

Evaluating the eigenvalues of $\boldsymbol{J}$, the modal frequency and damping may be described as:

$$\omega = \sqrt{Re(\lambda)^2 + Im(\lambda)^2} \quad \textbf{(Eq. 11)}$$

$$\xi = \frac{-Re(\lambda)}{\omega} \quad \textbf{(Eq. 12)}$$

Therefore, the mechanical system's stability regarding modal frequency and damping variation could be analyzed.

3. PIEZO-AEROELASTIC MODEL

In order to include the direct piezoelectric effect, the mechanical model must be adapted. The cantilever beam-based approach described by Erturk & Inman (2008) and De Marqui Jr et al. (2009) has been widely applied in several research. Although the main equations are presented here, the discussions and details can be found in their works.

The piezo-aeroelastic model rises from the linear aeroelastic equations of isotropic material and electro-elastic from piezoceramics subjected to aerodynamical loads. Additionally, it is considered that the piezoelectric material polarization in the structure occurs in a transverse direction, and the Kirchhoff plate hypothesis is applied to a system presented in Fig. 3.

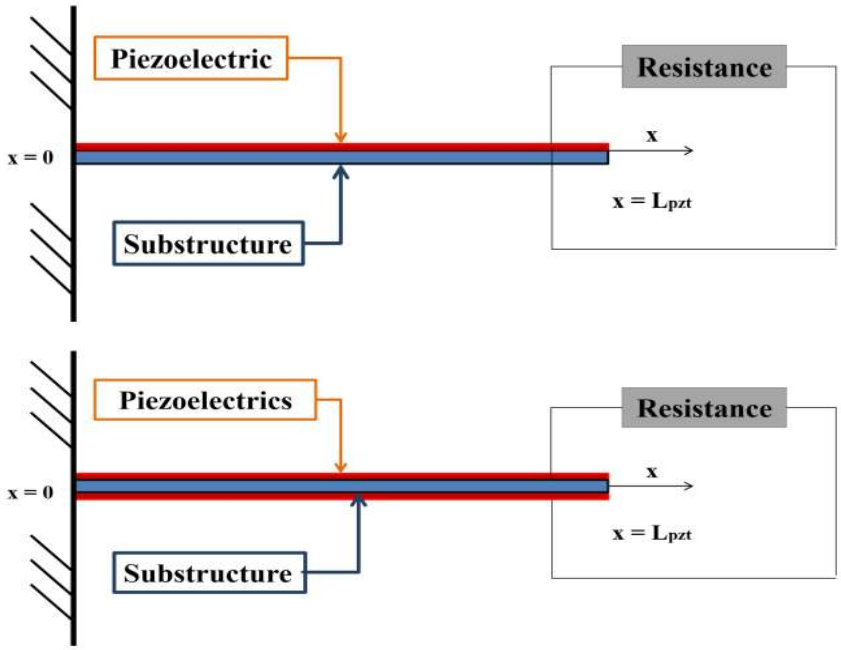


Figure 3. Piezoelectric couples in cantilever beams. At left, it is represented the unimorph harvester configuration. At right, the bimorph harvester one.

Thus, applying the Gaus law, the lumped model is given by (Abdelkefi, 2012) (Equations 13 and 14):

$$\boldsymbol{M\ddot{Y} + C\dot{Y} + KY - \Theta v_p = F} \qquad \textbf{(Eq. 13)}$$

$$\boldsymbol{C_p \dot{v}_p + \frac{v_p}{R_e} + \Theta^T \dot{Y} = 0} \qquad \textbf{(Eq. 14)}$$

Where $\boldsymbol{M}$, $\boldsymbol{K}$, $\boldsymbol{C}$ are the matrixes denoted as mass, stiffness, and damping. The

equivalent electromechanical matrix is $\boldsymbol{\Theta} = [\vartheta_\theta \quad \vartheta_\psi]^T$ and computes the direct piezoelectric effect in just only a single degree of freedom. The term v_p is the piezoelectric tension in the chosen DOF, C_p is the piezoceramic equivalent capacitance in the chosen DOF, $\boldsymbol{Y} = [\theta \quad \psi]^T$ is the displacement vector, R_e is external load resistance, and $\boldsymbol{F} = [M_\theta \quad M_\psi]^T$ is the force vector.

Due to the possibility of applying different types of piezoelectric material Cp and cursive tetamay be written in terms of piezoceramics' physical and geometric properties. Furthermore, it may use the same approach by Erturk & Inman (2008) to guarantee conformity to angular displacements. So, for *unimorph harvester* configuration, these terms could be written as **(Equations 15 – 20)**:

$$C_p = \frac{\varepsilon_{33}^S bL}{h_p} \quad \textbf{(Eq. 15)}$$

$$\vartheta = -\frac{Y_p b d_{31}}{2h_p}(h_c^2 - h_b^2) \quad \textbf{(Eq. 16)}$$

Where Y_p and d_{31} are, respectively, Young's modulus and a constant of piezoceramic. The terms b, h_p, and L are the w piezoelectric layer's width, thickness, and length, respectively. Additionally, ε_{33}^S is the permittivity. Also, note that if it is applied two piezoelectrics associated in series (*bimorph harvester case*), the electrical coupling is the same as the *unimorph* case. Nevertheless, the equivalent static capacitance will be half the case with a single piezoceramic (Erturk & Inman, 2009; De Marqui Jr. et al., 2009). Finally, h_c and h_b are the positions of the top and bottom of the piezoelectric layer from a neutral axis and are given, respectively, by:

$$h_b = h_{pa} - h_p \quad \textbf{(Eq. 17)}$$

$$h_c = h_{pa} \quad \textbf{(Eq. 18)}$$

once

$$h_{pa} = \frac{h_p^2 + 2n\, h_p h_s + n h_s^2}{2(h_p + n h_s)} \quad \textbf{(Eq. 19)}$$

with $n = {Y_s}/{Y_p}$, being Y_s the substructure Young's modulus and h_s the thickness of the substructure.

Therefore, the Jacobian matrix to piezo-aeroelastic system, $\boldsymbol{J_e}$, with a piezoceramic applied in only a single degree of freedom is given by:

$$\boldsymbol{J_e} = \begin{bmatrix} \mathbf{0_{2X2}} & \mathbf{1_{2X2}} & \mathbf{0_{2X1}} \\ -\boldsymbol{M^{-1}K} & -\boldsymbol{M^{-1}C} & \boldsymbol{M^{-1}\Theta} \\ \mathbf{0_{1X2}} & -{\boldsymbol{\Theta^T}}/{C_p} & -1/(R_e C_p) \end{bmatrix} \quad \textbf{(Eq. 20)}$$

Thus, evaluating the eigenvalues of **Eq. (20)**, the modal frequency and damping, including the direct piezoelectric effect, can be evaluated, allowing accessing the piezoelectric effects on the system's stability margin.

4. RESULTS

In order to observe the direct piezoelectric effect on the rotor-nacelle system, first it has been defined the physical and geometric parameters as depicted in **Tab. 1**.

Applying the description given by Erturk & Inman (2008), De Marqui Jr et al. (2009), Erturk & Inman (2009), and Abdelkefi (2012) in order to describe the piezoelectric coupling in terms of angular displacements and using the data presented in **Tab. 1** the effects on whirl-flutter aeroelastic behavior have been investigated through the software Matlab®. The eigenvalues have been obtained from Equations 10 and 20, and then the modal frequency and damping have been evaluated by **Equations 11 and 12**. So, considering the unimorph harvester configuration and applying the piezoelectric separately in the yaw and pitch DOF, **Fig. 4** has been obtained.

Table 1. Physical and Geometric System Properties

Parameters	**Values**
Length of piezoelectric, L	53,84 mm
Width of piezoelectric, b	20 mm
The thickness of the substructure, h_s	0,5 mm
The thickness of piezoelectric, h_p	0,4 mm
Young's modulus of substructure, Y_s	100 GPa
Young's modulus of piezoelectric, Y_p	66 GPa
Piezoelectric constant, d_{31}	-190 pm/V
Permittivity, ε_{33}^{S}	15,93 nF/m
Rotor radio, R	152 mm
Rotor angular velocity, Ω	40 rad/s
Pivot length to rotor radius ratio, a	0,25
Rotor moment of inertia, I_x	1,03 10^{-4} kg m^2
Nacelle moment of inertia, I_n	1,78 10^{-4} kg m^2
Structural pitch damping, c_θ	10^{-3} N m s/rad
Structural pitch stiffness, k_θ	0,4 N m/rad
Structural yaw damping, c_ψ	10^{-3} N m s/rad
Structural yaw stiffness, k_ψ	0,4 N m/rad
Number of blades, n_b	4
Blade chord, c	26 mm
Blade lift slope, $c_{l,\alpha}$	2π rad^{-1}

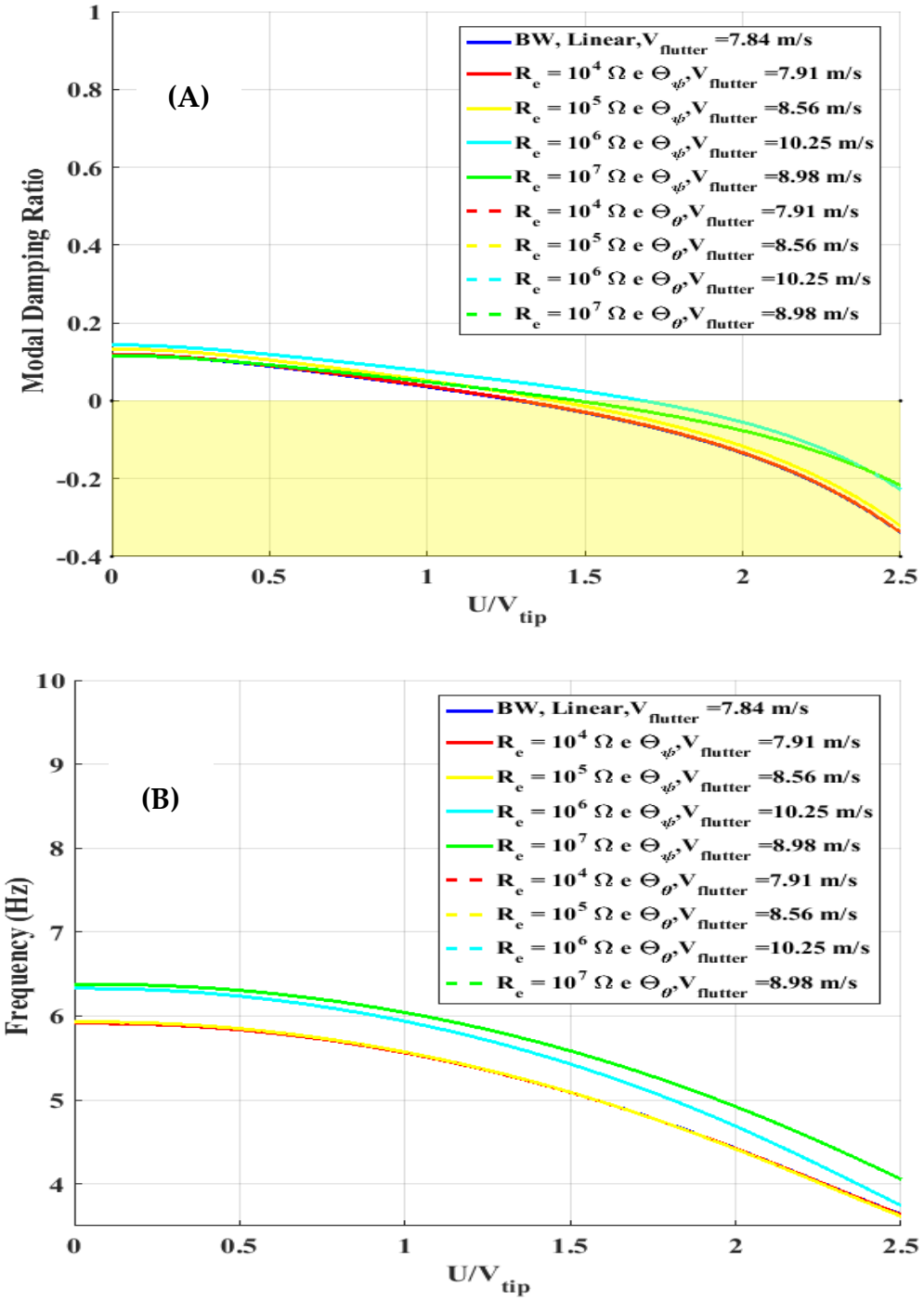
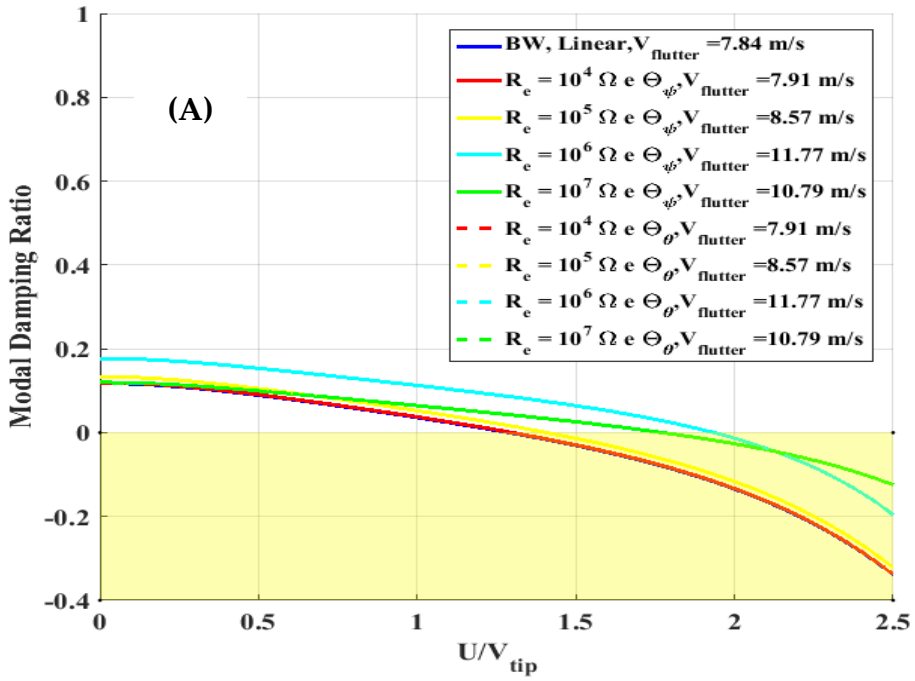


Figure 4. *Unimorph harvester* system's response. On the left is the modal damping ratio of pitch (solid) and yaw (dashed) (A), and ta the right is the modal frequency of pitch (solid) and yaw (dashed) variation (B).

As may be observed from the variation of the modal damping ratio of pitch and yaw motions in **Fig. 4a**, the linear mechanical system presented a critical speed, normalized by the tangential speed at the propeller tip of $U/Vtip$ = 1.29, which corresponds to U = 7.84 m/s. Including the electrical coupling with an external resistance $R_e = 10^4$ Ω, the flutter speed has been postponed to U = 7.91 m/s. Increasing the load resistance up to $R_e = 10^6$ Ω, the critical speed has also been

increased, achieving its maximum value U = 10.25 m/s. Nonetheless, when a higher load resistance has been applied, such as $R_e = 10^7\ \Omega$, the critical speed was reduced, achieving U = 8.98 m/s. The shunt-damping effect may explain such an increase in the range of stable speeds, directly affecting the system's stability margins. As depicted **in Fig. 4a**, the total damping is also enhanced as the external load resistance increases to the optimal value. With the structural motion, mechanical energy is converted to electricity via the direct piezoelectric effect. Due to the energy dissipation in the external circuit, additional damping is introduced in the structure, increasing, as a consequence, the flutter speed. Such a fact becomes essential to the vibration control since the stability margin is extended to higher speeds so that the structural integrity may be guaranteed until the new critical speed. Note also that due to aeroelastic interaction and the piezoelectric effect, a variation in the frequencies of pitch and yaw motions is also observed in **Fig. 4b**.

The results presented in Fig. 5 are obtained by applying the bimorph harvester configuration.



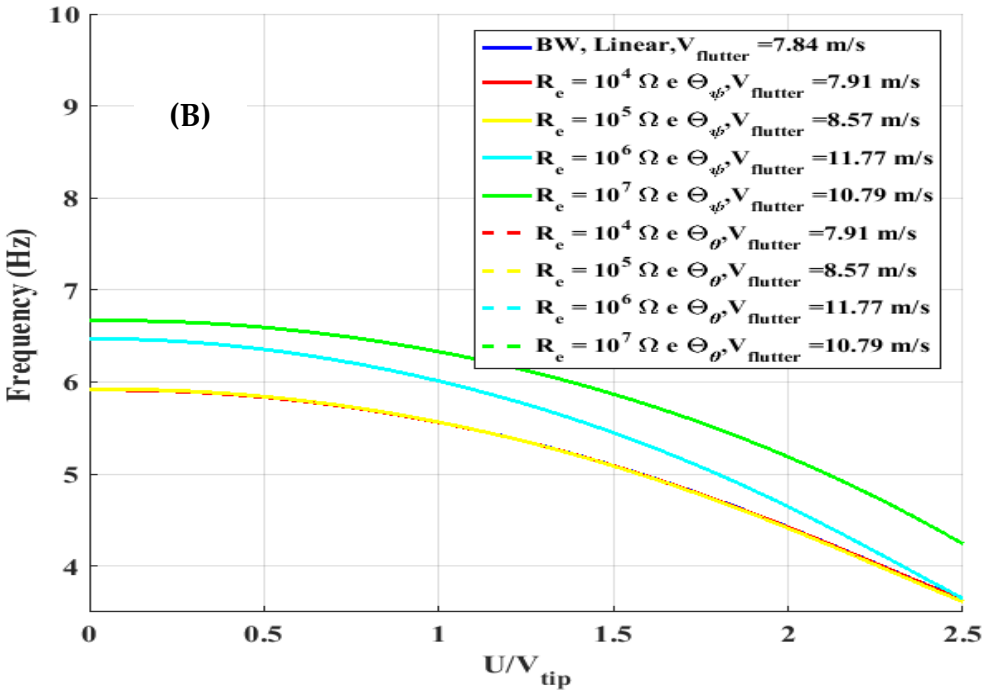


Figure 5. Bimorph harvester system's response. At left is the modal damping ratio (a), and ta right is the modal frequency variation (b).

Although, in this case, two identical piezoceramics are associated in series, a similar behavior, compared with the *unimorph* case, has been observed. Again, the observed optimal resistance was $R_e = 10^6\ \Omega$ which provides a flutter speed of U = 11.77 m/s higher, therefore, than the *unimorph* case. Moreover, considering the load resistance of $R_e = 10^7\ \Omega$, the critical speed has been reduced compared with the optimal case achieving U = 10.79 m/s. However, such speed is still higher than the *unimorph* optimal case, as depicted in **Fig. 5a**. Furthermore, due to the shunt damping effect and aeroelastic interactions, there was a higher variation in modal frequencies, as observed in **Fig. 5b**. All these effects are more pronounced due to the equivalent capacitance. As in the present case, the equivalent capacitance is half of a unique piezoceramic, and the system's capability to store power is half of the *unimorph* one. Therefore, as more energy is dissipated in the external circuit, the direct piezoelectric effect is more substantial, providing a higher shunt damping effect that causes, as a consequence, an increase in the structural damping and, as a consequence, a higher value of flutter speed, enhancing the stability margin when comparing with the *unimorph* configuration. In summary, the percentage gain in the stability margin for both *unimorph* and *bimorph* configurations is presented in **Tab. 2**.

Table 1. The percentage gain in the stability margins for both *unimorph* and *bimorph* configurations.

Resistance (Ω)	Unimorph	Bimorph
$R_e = 10^4$	0.89%	0.89%
$R_e = 10^5$	9.18%	9.31%
$R_e = 10^6$	30.74%	50.12%
$R_e = 10^7$	14.54%	37.63%

At last, it should be mentioned that the piezoelectric layer, either the yaw or pitch DOF, has provided the same system's response; once the dashed and the continuous lines represent the PZT application in the yaw and pitch DOF, respectively, are overlapped.

5. CONCLUSIONS

The present research analyzed the main effects of the whirl-flutter instability control applying piezoceramics in *unimorph* and bimorph configurations.

Applying different values of resistance, the optimal value for postponing the critical instability speed for both *unimorph* and *bimorph* configurations is $R_e = 10^6$ Ω. In the *unimorph* configuration, the flutter speed may be increased from U = 7.84 m/s to U = 10.25 m/s, representing an increase of 30.74%. In the *bimorph* configuration, up to U = 11.77 m/s, representing an increase of 50.12%. When a higher value of resistance has been applied, $R_e = 10^7$ Ω, the critical speed is reduced in comparison to the optimal case.

In all cases, such enhancement in the flutter speed occurs due to the shunt damping effect that increases the total damping. Once the structure is vibrating, the piezoelectric converts mechanical to electrical energy through the direct piezoelectric effect. When this energy is dissipated in an external circuit, the structural damping and the stability margins are increased. Until this new critical speed is achieved, the system's response is damped, and the structural integrity is guaranteed. In the *bimorph* case, these effects may be more pronounced due to the equivalent capacitance, which is half that of the *unimorph* case. When analyzing the frequency variation concerning freestream velocity, the piezoelectric effect works together with the aeroelastic effects in the frequency variation.

Finally, the system has a symmetrical behavior since applying the piezoceramics in the pitch or yaw DOF separately provided the same responses once the dashed and the continuous lines overlapped.

6. AUTHOR INFORMATION

Sérvio Túlio Suenai Haramura Bastos
Corresponding author. E-mail address: tulio.haramura@unesp.br

REFERENCES

(1) Abdelkefi, A. (2012). Global nonlinear analysis of piezoelectric energy harvesting from ambient and aeroelastic vibrations. [PhD diss., Virginia Polytechnic Institute and State University]. https://ui.adsabs.harvard.edu/abs/2012PhDT.....289A

(2) Abdelkefi, A. (2016). Aeroelastic energy harvesting: A review. International Journal of Engineering Science, (100), 112–135. http://dx.doi.org/10.1016/j.ijengsci.2015.10.006

(3) Abdelkefi, A., & Ghommem, M. (2013). Piezoelectric energy harvesting from morphing wing motions for micro air vehicles. Theoretical and Applied Mechanics Letters, 3(5), 052004. http://dx.doi.org/10.1063/2.1305204

(4) Abdelkefi, A., Hajj, M. R., & Nayfeh, A. (2012). Piezoelectric energy harvesting from transverse galloping of bluff bodies. Smart Materials and Structures, (22), 015014. http://dx.doi.org/10.1088/0964-1726/22/1/015014

(5) Abdelkefi, A., Nayfeh, A., & Hajj, M. R. (2011). Modeling and analysis of piezoaeroelastic energy harvesters. Nonlinear Dynamics, (67), 925–939. http://dx.doi.org/10.1007/s11071-011-0035-1

(6) Adeyemi, D. A., Cleaver, D. J., & Du Bois, J. L. (2019). Whirl flutter modelling for active control. [Conference Paper]. The 4th Annual UK Vertical Lift Network Technical Workshop, Cheshire. 2019. https://www.bath.ac.uk/publications/control-and-actuation-research-projects/attachments/active-control-of-whirl-flutter.pdf

(7) Akhras, G. (2000). Smart materials and smart systems for the future. Canadian Military Journal, 1(3), 25–31. http://www.journal.forces.gc.ca/vo1/no3/doc/25-32-eng.pdf

(8) Anicezio, M. M. (2015). Atenuação de vibrações em pás de helic´opteros utilizando circuito piezelétrico semi-passivo. [Master's thesis, University of Sao Paulo] https://doi.org/10.11606/D.18.2016.tde-30052016-162637

(9) Bastos, S. T. S. H., & Vasconcellos, R. M. G. (2021). Amplitude reduction through energy harvesting in vortex-induced vibrations. [Conference Paper]. International Conference on Advances in Energy Harvesting Technology. Virtual. 2021. https://repositorio.unesp.br/handle/11449/235718

(10) Bastos, S. T. S. H., & Vasconcellos, R. M. G. (2022a). Análise do comportamento aeroelástico da instabilidade de whirl-flutter em rotores de aeronaves. [Conference Paper]. XXVIII congresso nacional de estudantes de engenharia mecanica (creem 2022), Santa Maria. 2022. doi://10.26678/ABCM.CREEM2022.CRE2022-0022

(11) Bastos, S. T. S. H., & Vasconcellos, R. M. G. (2022b). Efeitos da aplicação de piezocerâmicas no comportamento aeroelástico de rotores submetidos ao whirl-flutter. [Conference Paper]. WPGEE - Workshop do Programa em Engenharia Elátrica ICTS/SJBV, São João da Boa Vista. 2022. https://repositorio.unesp.br/hdl.handle.net/11449/214041

(12) Bastos, S. T. S. H., Vasconcellos, R. M. G., & Marques, F. D. (2019a). Vibrações induzidas por vórtice em um cilindro com um grau de liberdade e rigidez não linear. [Conference Paper]. Congresso ibero-americano de engenharia mecânica - cibim, Cartagena. 2019. https://repositorio.unesp.br/handle/11449/235719

(13) Bastos, S. T. S. H., Vasconcellos, R. M. G., & Marques, F. D. (2019b). Vortex induced vibration in a single degree of freedom cylinder with structural nonlinearities. [Conference Paper]. 25th ABCM international congress of mechanical engineering cobem, Uberlandia. 2019. http://dx.doi.org/10.26678/ABCM.COBEM2019.COB2019-0769

(14) Bielawa, R. L. (2005). Rotary wing structural dynamics and aeroelasticity. AIAA education series. American Institute of Aeronautics and Astronautics. https://doi.org/10.2514/4.862373

(15) Čečrdle, J. (2015). Theoretical background of whirl flutter phenomenon. In Čečrdle, J. (Ed.). Whirl flutter of turboprop aircraft structures. (pp. 13–31). Woodhead Publishing. http://dx.doi.org/10.1533/9781782421863.13

(16) D'Assunção, D. (2013). Circuito piezelétrico chaveado para controle de vibrações e coleta de energia em uma seção típica aeroelástica. [Master's thesis, University of Sao Paulo]. https://doi.org/10.11606/D.18.2013.tde-18092013-144556

(17) De Marqui Jr, C., Erturk, A., & Inman, D. (2009). Piezoaeroelastically coupled modeling and

analysis of electrical power generation and shunt damping for a cantilever plate. [Conference Paper]. 17th International Conference on Composite Materials, Edinburgh, 2019. http://iccm-central.org/Proceedings/ICCM17proceedings/papers/B5.7%20De%20Marqui.pdf

(18) Erturk, A., & Inman, D. J. (2008). A distributed parameter electromechanical model for cantilevered piezoelectric energy harvesters. Journal of Vibration and Acoustics, 130(4), 041002. http://dx.doi.org/10.1115/1.2890402

(19) Erturk, A., & Inman, D. J. (2009). An experimentally validated bimorph cantilever model for piezoelectric energy harvesting from base excitations. Smart Materials and Structures, 18(2), 025009. http://dx.doi.org/10.1088/0964-1726/18/2/025009

(20) Karami, M. A., & Inman, D. (2012). Linear and nonlinear energy harvesters for powering pacemakers from heart beat vibrations. Applied Physics Letters, (100). http://dx.doi.org/10.1117/12.880168

(21) Kruger, W. R. (2016). Multibody analysis of whirl flutter stability on a tiltrotor wind tunnel model. Proceedings of the Institution of Mechanical Engineers, Part K: Journal of Multi-body Dynamics, 230(2), 121– 133. http://dx.doi.org/10.1177/1464419315582128

(22) Latif, R., Khan, M., Javed, A., Shah, S., & Rizvi, S. (2021). A semi-analytical approach for flutter analysis of a high-aspect-ratio wing. The Aeronautical Journal, 125(1284), 410–429. http://dx.doi.org/10.1017/aer.2020.71

(23) Liu Xu, V. (2020). Propeller-wing whirl flutter: an analytical approach. Mestrado em engenharia aeronáutica. [Master's thesis, Delft University of Technology]. . http://resolver.tudelft.nl/uuid:ac4b57c8-724f-43ce-871c-0bfc326874bb

(24) Mair, C., Rezgui, D., & Titurus, B. (2019). Stability analysis of whirl flutter in a nonlinear gimballed rotor-nacelle system. https://vtol.org/store/product/forum-75-proceedings-cdphiladelphia-pennsylvania-may-2019-14366.cfm

(25) Mair, C., Rezgui, D., & Titurus, B. (2018). Nonlinear stability analysis of whirl flutter in a rotor-nacelle system. Nonlinear Dynamics, (94), 2013-2032. http://dx.doi.org/10.1007/s11071-018-4472-y

(26) Mair, C., Titurus, B., & Rezgui, D. (2021). Stability analysis of whirl flutter in rotor-nacelle systems with freeplay nonlinearity. Nonlinear Dynamics, (104), 1–25. http://dx.doi.org/10.1007/s11071-021-06271-z

(27) Mueller, J., Gourinat, Y., Ferrer, R., K. T., & Kerdreux, B. (2004). A numerical study on active control for tiltrotor whirl flutter stability augmentation. [Conference Paper]. American Helicopter Society 4th Decennial Specialist's Conference on Aeromechanics, San Francisco, 2004. https://doi.org/10.4050/1.3092885

(28) Muralt, P. (2000). Ferroelectric thin films for micro-sensors and actuators: A review. Journal of Micromechanics and Microengineering, (10), 136-146. http://dx.doi.org/10.1088/0960-1317/10/2/307

(29) Naseer, R., Dai, H., Abdelkefi, A., & Wang, L. (2017). Piezomagnetoelastic energy harvesting from vortex-induced vibrations using monostable characteristics. Applied Energy, (203), 142–153. http://dx.doi.org/10.1016/j.apenergy.2017.06.018

(30) Piatak, D., Kvaternik, R., Nixon, M., Langston, C., Singleton, J.D., Bennett, R., & Brown, R. (2003). A wind-tunnel parametric investigation of tiltrotor whirl-flutter stability boundaries. [Conference Paper]. American Helicopter Society 57th Annual Forum, Washington, 2003. https://ntrs.nasa.gov/api/citations/20010057781/downloads/20010057781.pdf?attachment=true

(31) Quintana, A., Vasconcellos, R., Throneberry, G., & Abdelkefi, A. (2021). Nonlinear analysis and bifurcation characteristics of whirl flutter in unmanned aerial systems. Drones, 5(4). http://dx.doi.org/10.3390/drones5040122

(32) Reed III, W. H. (1966). Propeller-rotor whirl flutter: A state-of-theart review. Journal of Sound and Vibration, (4), 526–544. https://doi.org/10.1016/0022-460X(66)90142-8

(33) Ribner, H. S. (1945a). Formulas for propellers in yaw and charts of the side – force derivatives. Technical report, NASA Langley Technical Report

Server. https://ntrs.nasa.gov/citations/19930091896

(34) Ribner, H. S. (1945b). Propellers in yaw. Technical report, NASA Langley Technical Report Server. https://ntrs.nasa.gov/citations/19930091897.

(35) Roundy, S., & Wright, P. (2004). A piezoelectric vibration based generator for wireless electronics. Smart Materials and Structures, (13), 1131. http://dx.doi.org/10.1088/0964-1726/13/5/018

(36) Silva, T. M. P. (2014). Circuitos piezelétricos passivos, semipassivos, ativos e híbridos e suas aplicações para problemas aeroelásticos. [Master's thesis, University of Sao Paulo]. https://doi.org/ 10.11606/D.18.2017.tde-16112017-112104

(37) Taylor, E. S., & Browne, K. A. (1938). Vibration isolation of aircraft power plants. Journal of the Aeronautical Sciences, 6(2), 43–49. http://dx.doi.org/10.2514/8.760

(38) Vasconcellos, R., & Abdelkefi, A. (2015). Nonlinear dynamical analysis of an aeroelastic system with multi-segmented moment in the pitch degree-of-freedom. Communications in Nonlinear Science and Numerical Simulation, (20), 324-334. http://dx.doi.org/10.1016/j.cnsns.2014.05.017